Photoexcitation and Photoionization Dynamics of Water Photolysis

Anupriya Kumar,[†] Maciej Kołaski,[†,‡] Han Myoung Lee,[§] and Kwang S. Kim*[,†]

Center for Superfunctional Materials and Basic Science Research Institute, Department of Chemistry, Pohang University of Science and Technology, San 31, Hyojadong, Namgu, Pohang 790-784, Korea

Received: December 5, 2007; Revised Manuscript Received: March 25, 2008

Despite the importance of water photolysis in atmospheric chemistry, its mechanism is not well understood. Two different mechanisms for water photolysis have been proposed. The first mechanism is driven by water photoexcitation, followed by the reaction of the active hydrogen radical with water clusters. The second mechanism is governed by the ionization process. Both photoexcited and photoionized mechanisms are complementary, which is elucidated by using excited-state ab initio molecular dynamics simulations based on complete active space self-consistent field approach and unrestricted Møller−Plesset second-order perturbation theory based Born−Oppenheimer molecular dynamics simulations.

Introduction

Photodissociation is a chemical process in which a chemical compound is dissociated by light (photons). Photolysis plays an important role in many chemical[1,2] and atmospheric phenomena.[3] In the earth's atmosphere, photolysis occurs as part of a series of reactions by which primary pollutants (such as hydrocarbons and nitrogen oxides) react to generate secondary pollutants (e.g., peroxyacyl nitrates).[4] In the stratosphere, ozone is formed through photolysis by UV light.[5] Chlorofluorocarbons (CFCs) are broken down by photolysis in the uppermost atmosphere to form chlorine-free radicals, which destroy the ozone layer.[6] In astrophysics, photodissociation is one of the major processes through which molecules are broken down (but new molecules are being formed).[3] It was suggested that methane observed on Mars can be formed by photolysis of water vapor in the presence of carbon monoxide.[7] The photolysis of water is also important in neutron irradiation to the cooling water in nuclear reactor technology and in the damage of living cells caused by radiation. What is more important is that one possible fuel source may be obtained via the photolysis of water to hydrogen and oxygen gases.[8]

Despite the importance of water photolysis as described above, the mechanism for water photolysis is still not well understood.[9] Two different mechanisms of water photolysis have been proposed:

(1) Upon excitation, a water molecule forms $OH^{\bullet}$ and $H^{\bullet}$ radicals, and the excess energy is kept mainly on the $H^{\bullet}$ radical. Subsequently, the $H^{\bullet}$ radical has large kinetic energy and immediately reacts with a water molecule in the first hydration shell, forming H_3O^+ and the hydrated electron.[10–12]

$$H_2O + h\nu \rightarrow H_2O^* \rightarrow H^{\bullet} + OH^{\bullet} \quad (1)$$

$$H^{\bullet}\,(\text{hot}) + H_2O \rightarrow H_3O^+ + e^-\,(\text{hydrated}) \quad (2)$$

This mechanism is controlled by photoexcitation. While the hot hydrogen radicals are formed, they directly generate the H_3O^+ and hydrated electrons.

(2) It has been suggested that the ionization above the Born−Oppenheimer threshold leads to formation of the H_3O^+, $OH^{\bullet}$ radical, and hydrated electron.[11,13–16]

$$H_2O + h\nu \rightarrow H_2O^+ + e^-\,(\text{hydrated}) \quad (3)$$

$$H_2O^+ + H_2O \rightarrow H_3O^+ + OH^{\bullet} \quad (4)$$

Contrary to the previous mechanism, in case (2), the reaction is caused by photons with energies above the ionization threshold. Namely, in the first case, the photolysis is driven by photoexcitation, while in the second case the reaction is governed by the ionization process. However, both schemes lead to the same products, while their reaction mechanisms are significantly different.

The UV spectrum of a water molecule comprises two broad bands with maxima at 165 (7.5 eV) and 128 nm (9.7 eV).[17] They correspond to the following singlet electronic transitions: $1\,^1A_1 \rightarrow 1\,^1B_1$ and $1\,^1A_1 \rightarrow 2\,^1A_1$. The $1\,^1A_1 \rightarrow 1\,^1B_1$ transition corresponds to the highest occupied molecular orbital (HOMO) to lowest unoccupied molecular orbital (LUMO) excitation, and the $1\,^1A_1 \rightarrow 2\,^1A_1$ transition is assigned to the second HOMO (HOMO−1) to LUMO excitation. The ratio of dissociation caused by $1\,^1A_1 \rightarrow 1\,^1B_1$ to that caused by $1\,^1A_1 \rightarrow 2\,^1A_1$ is 0.89:0.11,[17d] which indicates that the HOMO−LUMO excitation is dominant. The ionization energy of water molecule in the gas phase is 12.6 eV,[18,19] which is considerably larger than the corresponding excitation energies from water in the UV spectrum. Thus, if the energy of photon is above the ionization threshold, the mechanism is determined by the ionization.

The water clusters [20–26] have been theoretically studied extensively; in most of the cases the structures, binding energies, electron affinities, and infrared spectra have been calculated.[20–28] The study of water photolysis requires molecular dynamics simulations based on intramolecular interactions. In this regard, we report the photoexcitation mechanism by using excited-state (ES) ab initio molecular dynamics (AIMD) simulations based on complete active space self-consistent field (CASSCF) formalism and the photoionization mechanism by using the ground-state unrestricted Moller−Plesset second-order perturbation theory (MP2) based Born−Oppenheimer molecular dynamics (BOMD) simulations. We believe that this is the first systematic report of water photolysis mechanisms based on ES-AIMD and unrestricted MP2-BOMD simulations.

* Corresponding author. E-mail: kim@postech.ac.kr.
† Center for Superfunctional Materials.
‡ Permanent address: Department of Theoretical Chemistry, Institute of Chemistry, University of Silesia, 9 Szkolna Street, 40-006 Katowice, Poland.
§ Basic Science Research Institute.

10.1021/jp711485b CCC: $40.75
Published on Web 05/28/2008

TABLE 1: Excitation Energies (in eV) of the Water Molecule Calculated by Using Different Levels of Theory and Different Basis Sets[a]

	CIS (*f*)	TD-DFT (*f*)	CAS-SCF	CAS-PT2	SAC-CISD (*f*)	EOM-CCSD (*f*)
			aVDZ			
$1\ ^1A_1 \rightarrow 1\ ^1B_1$	8.77	6.87	8.18	7.52	7.61	7.41
	(0.053)	(0.050)	9.29	9.75	(0.058)	(0.057)
$1\ ^1A_1 \rightarrow 2\ ^1A_1$	11.04	9.04			9.91	9.84
	(0.105)	(0.087)			(0.102)	(0.104)
			aVTZ			
$1\ ^1A_1 \rightarrow 1\ ^1B_1$	8.79	6.91	8.20	7.61	7.72	7.60
	(0.053)	(0.047)	9.23	9.84	(0.053)	(0.054)
$1\ ^1A_1 \rightarrow 2\ ^1A_1$	11.04	9.03			9.99	9.95
	(0.105)	(0.081)			(0.094)	(0.099)
			aVQZ			
$1\ ^1A_1 \rightarrow 1\ ^1B_1$	8.82	6.92	8.21	7.69	7.77	7.68
	(0.050)	(0.046)	9.19	9.86	(0.051)	(0.052)
$1\ ^1A_1 \rightarrow 2\ ^1A_1$	11.01	9.03			10.00	10.01
	(0.095)	(0.078)			(0.088)	(0.095)

[a] The experimental excitation energies of $1\ ^1A_1 \rightarrow 1\ ^1B_1$ and $1\ ^1A_1 \rightarrow 2\ ^1A_1$ are 7.82 and 9.69 eV, respectively.[17] The geometries used are as follows: [CIS: HF-optimized geometry; TD-DFT: B3LYP-optimized geometry, CASSCF: CASSCF-optimized geometry, CASPT2: CASPT2-optimized geometry, SAC-CISD: HF geometry, and EOM-CCSD: CCSD-optimized geometry].

Computational Methods

We performed some test calculations (excitation energies and ionization potential) for a single water molecule using different computational approaches and various basis sets such as aug-cc-pVDZ (abbreviated as aVDZ), aug-cc-pVTZ (aVTZ), and aug-cc-pVQZ (aVQZ). As shown in Table 1, the excitation energies based on CASSCF, complete active space with second-order perturbation theory (CASPT2), symmetry-adapted cluster configuration interaction with single and double excitations (SAC-CISD), equation of motion coupled cluster with single and double excitations (EOM-CCSD) are in good agreement with the experimental results. However, the configuration interaction with single excitations (CIS) tends to overestimate excitation energies and the time-dependent density functional theory (TD-DFT) approach tends to underestimate them. The CASSCF method, though low level of theory, gives reasonable values for the excitation energies possibly because of the cancelation effect of the dynamic correlation in this system. The oscillator strengths for CIS, TD-DFT, SAC-CISD, and EOM-CCSD at aVDZ/aVTZ/aVQZ basis sets for the transition $1\ ^1A_1 \rightarrow 1\ ^1B_1$ are 0.053/0.053/0.050, 0.050/0.047/0.046, 0.058/0.053/0.051, and 0.057/0.054/0.052. The oscillator strengths for CIS, TD-DFT, SAC-CISD, and EOM-CCSD at aVDZ/aVTZ/aVQZ basis sets for state $1\ ^1A_1 \rightarrow 2\ ^1A_1$ are 0.105/0.105/0.095, 0.087/0.081/0.078, 0.102/0.094/0.088, and 0.104/0.099/0.095. For this water photolysis, the basis set effect is not large. For larger basis sets, the excitation energies are close to those calculated with the aVDZ basis set; the maximum difference does not exceed 0.2 eV as shown in Table 1. The first vertical excitation energies calculated without using the symmetry for the water monomer, dimer, and trimer at the CASSCF/aVDZ level are 8.18, 9.55, and 9.21 eV, respectively. The vertical ionization potentials of the water monomer, dimer, and trimer at the CASSCF/aVDZ level are 10.98, 11.30, and 11.04 eV, respectively, and those at the MP2/aVDZ [CCSD(T)/aVDZ] level are 12.70 [12.51], 11.80 [11.62], and 12.32 [12.09] eV, respectively. Thus, the ionization energies of the water monomer, dimer, and trimer are 2.80, 1.75, and 1.83 eV higher than the corresponding vertical excitation energies at the CASSCF/aVDZ level. The vertical ionization potential of the water monomer was also calculated at density functional theory (DFT) level with Becke's three-parameter exchange potential and the Lee−Yang−Parr correlation functional (B3LYP) as well as UMP2 and coupled cluster with single, double, and perturbative triple excitation (CCSD(T)) levels of theory by using aVDZ, aVTZ, and aVQZ basis sets as shown in Table 2. All the excitation and vertical ionization energies were calculated by using the MOLPRO package.[29]

TABLE 2: Vertical Ionization Potential (in eV) of the Water Molecule Calculated by Using Different Levels of Theory and Different Basis Sets[a]

	B3LYP	MP2	CCSD(T)
aVDZ	12.78	12.70	12.51
aVTZ	12.78	12.86	12.67
aVQZ	12.80	12.93	12.73

[a] The experimental value is 12.59 eV.[18] All the geometries were optimized.

In this regard, the ES-AIMD simulations[30] of the water photolysis were carried out by using the CASSCF/aVDZ method, as a necessary compromise between the desired accuracy and the computational cost. The simulations were performed by using the HONDO suite of programs.[31] In the case of UMP2-BOMD simulations, the ionization potential calculated at the UMP2 level is close to the experimental value.

In ES-AIMD simulations, the choice of the active space is crucial. For a water molecule, we used the active space (6,6). We also performed test calculations using full-valence active space (8,8). We found that both dynamics are almost identical. For the water dimer, the (12,12) active space was exploited. For the water trimer, we employed the same active space, as in the case of the water dimer. The optimal choice of the active space is critical for the reduction of computational resources, even though the computational accuracy is slightly sacrificed. It is important to note that, in the case of ES-AIMD simulations, the MOs involved in the photoexcitation process should be present in the active space. In this ES-AIMD simulation, we considered the first single excitations (i.e., HOMO−LUMO excitations). At the CASSCF level, the dynamical correlation effects were not taken into account. Thus, the dispersion energy cannot be properly recovered at this level of calculations. AIMD simulations based on the CASPT2 method should be more reliable. However, CASPT2 is computationally very demanding and in many cases diverges due to the "intruder state" problem.[35] We performed single-point CASPT2 calculations for selected

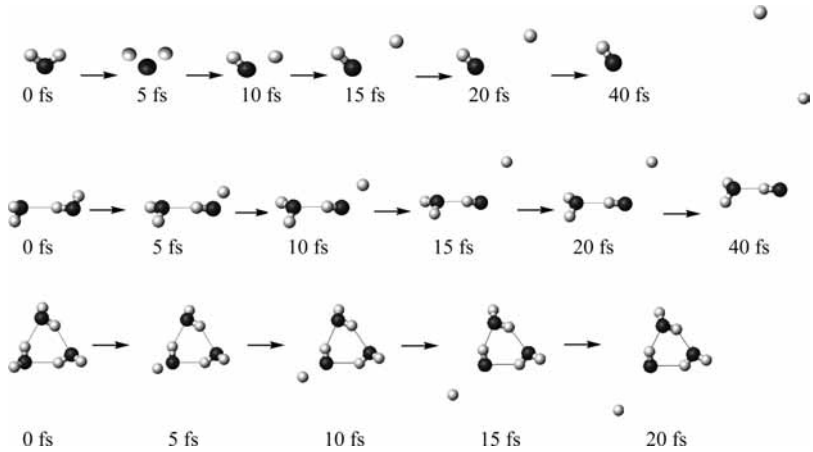

Figure 1. Snapshots of the evolving process of $(H_2O)_{n=1-3}$ clusters upon the excitation (AIMD simulations).

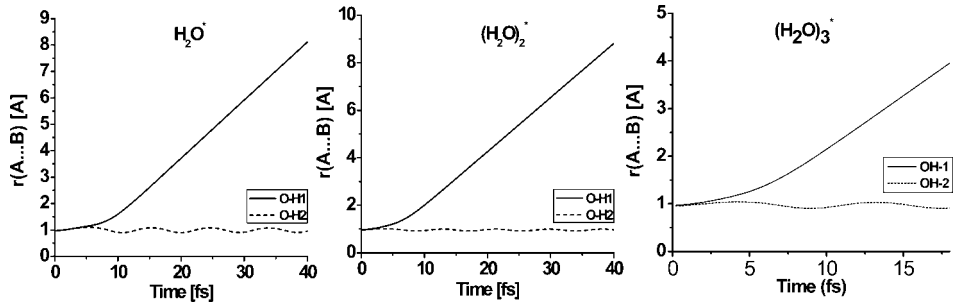

Figure 2. Time evolution of distances for excited $(H_2O)_{n=1-3}$.

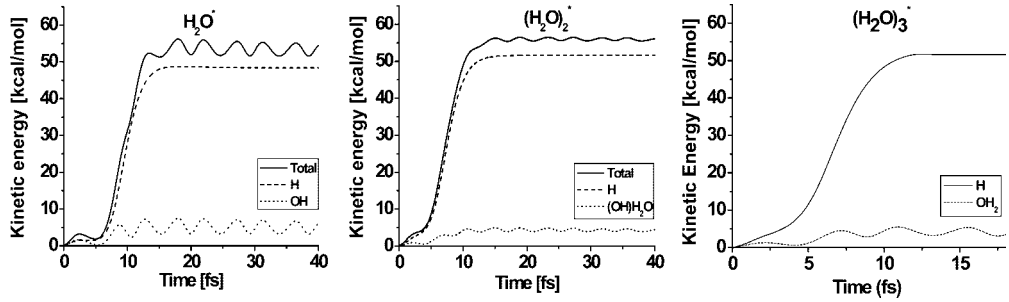

Figure 3. Time evolution of kinetic energy components for excited $(H_2O)_{n=1-3}$.

geometries of the $(H_2O)_{n=1-3}$ clusters. We found that the energy changes in the CASSCF approach were similar to those in the CASPT2 approach, because the dynamical correlation energies for the same size of clusters were almost equivalent. The differences between CASSCF and CASPT2 binding energies for H_2O, $(H_2O)_2$, and $(H_2O)_3$ are 0.14, 0.32, and 0.53 eV, respectively, and these values remain almost constant unless the structures are changed significantly. Therefore, as the structures of clusters change with respect to time, both CASSCF and CASPT2 show almost the same energy changes, so that the CASSCF results are reliable in the present systems.

The initial structures having the ground-state minimum-energy geometry (optimized at the CASSCF/aVDZ level) were vertically excited. The ES-AIMD simulations of the water clusters were carried out for 40 fs with a time step of 0.1 fs. We also performed longer simulations, but all significant changes take place during the first 20 fs. Given that the experiments were done at low temperatures, we set the initial kinetic energies (KEs) to zero. In this case, the excitation energies of the $(H_2O)_{n=1-3}$ clusters (8.18, 9.55, 9.21 eV, respectively) are so large that the initial KEs of the clusters (0.08, 0.16, and 0.27 eV, respectively) do not contribute significantly to the dynamics. Thus, 0 K results should be almost the same with the average values of the 300 K ensembles. This has been demonstrated from the 24 sets of ES-AIMD simulations of the water monomer at 300 K, as shown in Figure 6. In this case, the geometries of the water monomer were selected for every 50 fs from the 1.2 ps CASSCF simulation of the ground-state water monomer at 300 K after 1 ps equilibration, and the initial velocities satisfying the Maxwell−Boltzmann distribution were randomly assigned for each simulation. Then, each system was excited for the ES-AIMD simulations.

In the case of UMP2-BOMD simulations for ionized water clusters, the initial Møller−Plesset second-order perturbation theory optimized minimum energy structures of neutral clusters were employed. We set the initial KEs to zero, as in the previous case. The UMP2-BOMD simulations were carried out for 1000 fs with a time step of 0.2 fs.

In the present study, both ES-AIMD (CASSCF/aVDZ) and ground-state BOMD (UMP2/aVDZ) simulations were carried out. Ground-state BOMD simulations (300 fs) for ionized water clusters were previously calculated at the HF/6−311G** level of theory.[32] However, no excited-state AIMD simulations have been reported on the photoexcitation of water clusters. We

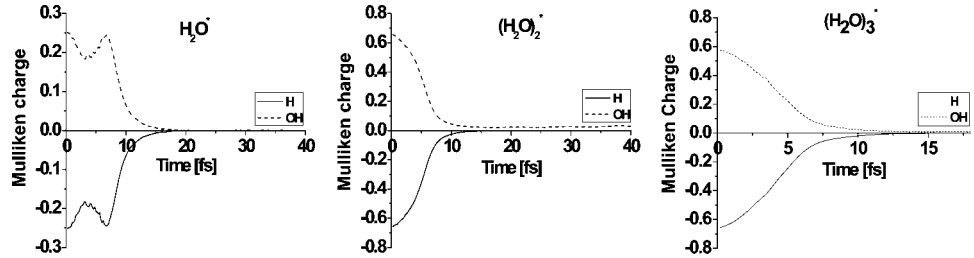

Figure 4. Time evolution of Mulliken charges for excited $(H_2O)_{n=1-3}$.

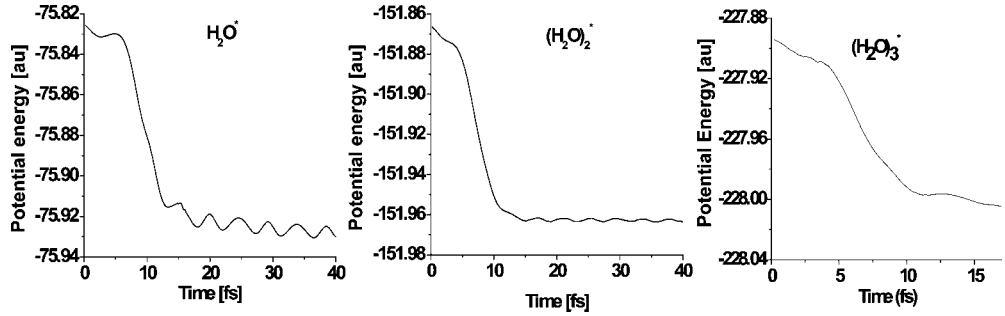

Figure 5. Time evolution of potential energy for excited $(H_2O)_{n=1-3}$.

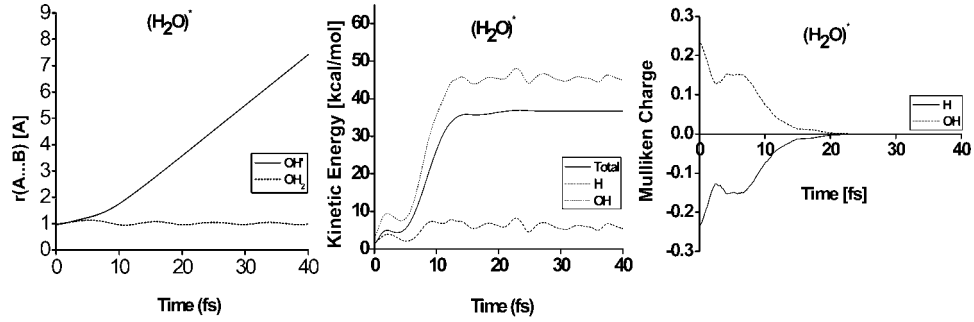

Figure 6. Sampling results of the time evolution of distances, kinetic energy components, and Mulliken charges for excited H_2O with initial kinetic energy at 300 K.

analyzed both dynamics in terms of the time evolution of structures, charges, kinetic energies, and potential energies. The charge analysis of the excited states (in ES-AIMD simulations) was made in Mulliken charges, while that of the ground states (in BOMD simulations) was made in natural bond orbital (NBO) charges.[33]

Results and Discussion

A. ES-AIMD Studies of Small Water Clusters. In the beginning of the ES-AIMD simulation, the dynamics of a single water molecule differs from dynamics of larger water clusters. Figure 1 shows the time evolution of the trajectories of conformational changes of the water clusters $(H_2O)_{n=1-3}$. In the beginning of the simulations, very strong O−H stretching motions are observed, and both OH bonds started to stretch (Figure 2) at ∼5 fs. At ∼10 fs, one hydroxyl group is formed again, and the hydrogen radical is detached from the water molecule. Its kinetic energy (Figure 3) grows very rapidly to ∼55 kcal/mol. The detached hydrogen radical has very large kinetic energy (∼50 kcal/mol, so it is very hot), which is consistent with the photoexcitation mechanism of the water photolysis. The analysis of Mulliken charges (Figure 4) localized on H and OH shows that, after 18 fs of simulations, the hydrogen and the hydroxyl group form radicals. In the beginning of AIMD simulations, the charges fluctuate because of strong vibrations of OH bonds. After ∼18 fs, the total charges localized on H and OH are zero. The analysis of the time evolution of the potential energy (Figure 5) shows that around 18 fs the minimum energy structure with H• and OH• is formed, which explains the maximum value of the total kinetic energy at 18 fs. The kinetic energy oscillates with rotational and vibrational motions along with the H-detached structure $OH-(H_2O)_{n=1,2}$. For these small water clusters, the H• radical releases within ∼15 fs (practically in ∼12 fs, and completely in ∼15 fs). The time evolutions of OH bond distances, kinetic energies, and charges obtained from the sampling of 24 different trajectories with the initial kinetic energy at 300 K for H_2O are shown in Figure 6,

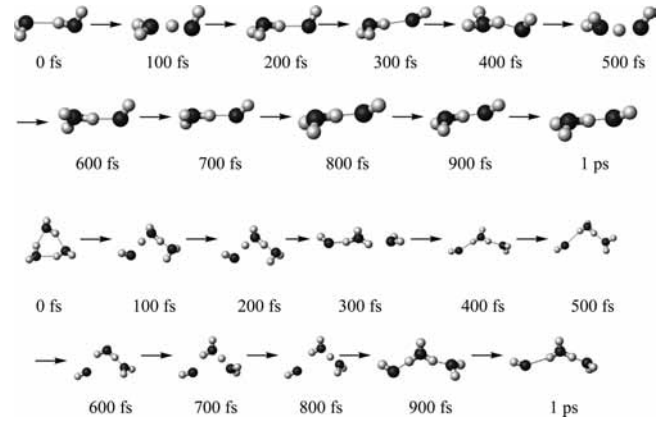

Figure 7. Snapshots of the evolving process of $(H_2O)^+_{n=2,3}$ clusters upon the photoionization of $(H_2O)_{n=2,3}$ (BOMD simulations).

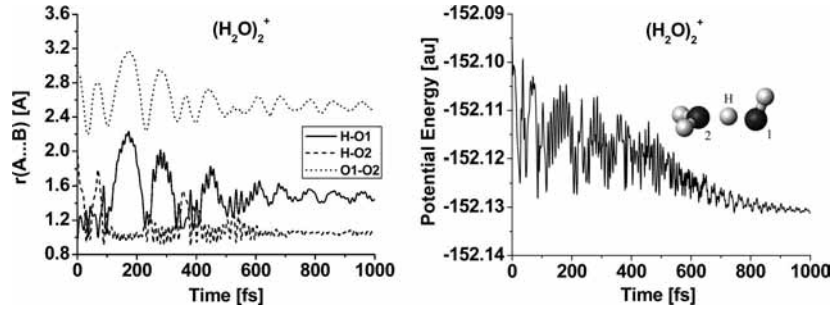

Figure 8. Time evolution of distances and the potential energy for the ionized water dimer.

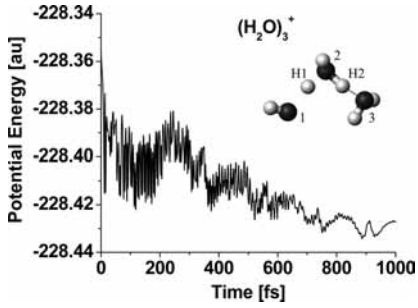

Figure 9. Time evolution of the potential energy for the ionized water trimer.

and they are almost similar to the graphs obtained from the simulation at 0 K. This is because for the water monomer the excitation energy is 7.82 eV, while the thermal energy is only 0.08 eV.

For the water dimer, the OH bond started to stretch at ~4 fs (Figure 2), and subsequently, the hydrogen is released from the system with very large velocity. While the OH bond is broken, the kinetic energy of the detached hydrogen grows very quickly. After 10 fs, the kinetic energy of the hydrogen radical (Figure 3) increases to ~55 kcal/mol and remains constant during the MD run. Upon the excitation, the hydrogen radical is negatively charged (−0.7e), while the hydroxyl group is positively charged (+0.7 e) as depicted in Figure 4. After 10 fs of the AIMD run, the negative charge localized on the hydrogen atom is completely transferred to the hydroxyl group; thus, H and OH become radicals. The charge does not fluctuate during the MD run because the strong stretching vibrations of OH bond are not observed during simulations. When the hydrogen radical is released, the hydroxyl radical and the adjacent water molecule form a stable structure.

The ES-AIMD simulation for the water trimer is similar to the photolysis of the water dimer. We report only 18 fs of the simulation, since the total energy is not conserved after 18 fs because of the mixing of orbital levels. The OH bond stretches at ~5 fs (Figure 2). During 10 fs, the kinetic energy of the detached hydrogen (Figure 3) grows very rapidly to ~55 kcal/mol. The total charge (Figure 4) localized on the H and OH radical groups becomes zero around 12 fs. During simulations, the cyclic ring is not open but one hydrogen bond is broken, and the cyclic ring is converted to a quasi-cyclic ring.

B. UMP2-BOMD Studies of Small Water Clusters. In the case of BOMD simulations for ionized water clusters, the structural changes are slower in comparison with ES-AIMD simulations. Thus, for ionized water clusters, we carried out 1000-fs BOMD simulations. The mechanism for water photolysis for ionized water clusters significantly differs from the photolysis driven by photoexcitation.

For the ionized water dimer, the proton oscillates between the hydroxyl group and the neighboring water molecule. The mobile proton has large kinetic energy; however, it does not exceed 10 kcal/mol, which holds the proton between the two oxygen atoms because the kinetic energy is not large enough to release the hydrogen atom from the cluster. The time evolution of H···O1 and H···O2 distances clearly indicates that Eigen (H_3O^+-like water cluster) and Zundel ($H_2O\cdots H^+\cdots OH_2$-like water cluster) forms[34] compete, as shown in Figure 7 (where each intercrossing represents the Zundel form). After 500 fs of simulations, an Eigen form is created, which is energetically more favorable. While the stable Eigen conformer is formed, the kinetic energy of the mobile proton substantially decreases. Figure 8 shows that the O1···O2 distance oscillates highly in the beginning of the simulations, but after 500 fs it does not change significantly. The time evolution of potential energy, shown in Figure 8, for an ionized water dimer confirms that the resulting structure is the minimum energy conformer. The analysis of the NBO charges shows that the positive charge localized on the OH group significantly changes during the MD run. In the beginning of the simulations, the hydroxyl group has charge +0.4e, which decreases to +0.1e at the end of the dynamics. The NBO charge of the mobile proton is almost constant (+0.6e) during simulations. The water molecule denoted as H_2O-2 is almost neutral at 0 fs, but after ~300 fs there is a charge transfer from the OH group to H_2O-2. However,

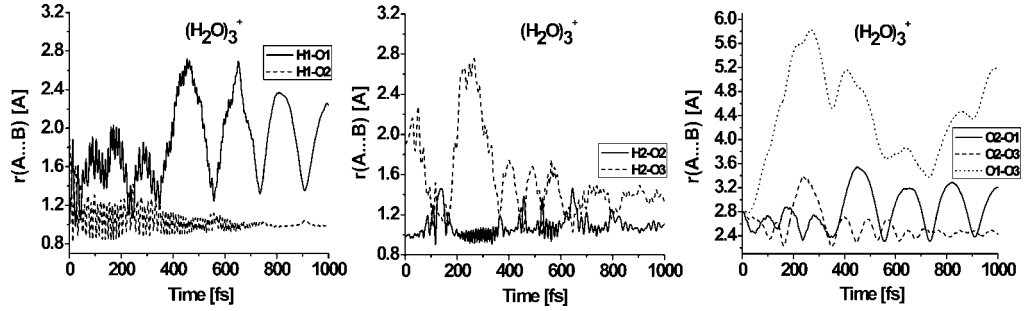

Figure 10. Time evolution of distances for the ionized water trimer.

the partial charge localized on OH is very small, while the hydroxyl radical is highly polarized by the neighboring hydronium cation.

The BOMD simulation for the ionized water trimer (Figure 7) slightly differs from the dynamics of the ionized water dimer. In the former case, the hydrogen atoms denoted as H1 and H2 oscillate between water molecules. In the beginning of the simulations, the dynamics is driven by H1 because H1 has larger kinetic energy than H2. During the first 500 fs, the Eigen and Zundel forms compete, similar to the case of the ionized water dimer. The geometry of the water trimer is completely altered during MD simulations. The cyclic ring is converted to a quasi-linear chain; moreover, at 300 fs the structure is almost linear. After 500 fs, the H1 hydrogen is bound to H_2O-2. After the proton transfer, the hydronium cation is formed. It is important to note that the hydronium cation comprises H1 and H2 atoms. While the H1 hydrogen is anchored to H_2O-2, the kinetic energy of H2 is still large (~5 kcal/mol); thus, H2 is moving between H_2O-2 and H_2O-3. After 800 fs of simulations, the kinetic energies of mobile hydrogen atoms decrease, and the system becomes stable. The kinetic energy ends up into the relative motion of water molecules in the vibrationally excited cluster. However, the resulting structure is not the minimum energy structure. In Figure 9, the time evolution of potential energy shows that during the last 200 fs the potential energy slightly oscillates because of small geometrical changes in the ionized water trimer. The analysis of NBO charges shows that in the beginning the hydroxyl group has some partial positive charge (+0.4e), but after 500 fs of MD simulations the OH radical is formed. The NBO charge localized on H_2O-3 fluctuates between 0 and +0.2e. At the end of simulations, the interatomic distance between O2 and O3 is around 2.4 Å as shown in Figure 10, which indicates that the cationic short hydrogen bond is formed between the hydronium cation and H_2O-3.

Concluding Remarks

This work reports the first ab initio excited-state molecular dynamics results to unravel the mechanism of water photolysis. Two different mechanisms were studied. Here, we confirmed that both mechanisms are complementary. The first mechanism is driven by photoexcitation phenomenon. Using ES-AIMD simulations based on the CASSCF approach, we showed that, upon excitation, water clusters release hot hydrogen radicals and (hydrated) hydroxyl radicals within 15 fs. In the case of water photolysis driven by ionization, all structural changes are slower in comparison with the dynamics controlled by the photoexcitation because of the lack of the hot $H^{\bullet}$ radical to be released. In ionized water clusters, the hydrogen atoms involved in hydrogen bond formation determine the structural reorganization of water clusters. In the beginning of simulations, these mobile protons have large kinetic energy, and thus Eigen and Zundel forms compete. After 500 fs, one proton is transferred to the adjacent water molecule, and the hydronium cation and $OH^{\bullet}$ radical are formed.

Acknowledgment. This work was supported by the GRL project (KICOS) and partly by the BK21 (KRF) program. Calculations were carried out using supercomputers in KISTI.

References and Notes

(1) (a) Ashfold, M. N. R., Baggott, J. E., Eds. *Molecular Photodissociation Dynamics*; Advances in Gas-Phase Photochemistry and Kinetics; Royal Society of Chemistry: London, 1987. (b) Pichat, P. *Water Sci. Technol.* **2007**, *55*, 167.

(2) (a) Hurley, S. M.; Dermota, T. E.; Hydutsky, D. P.; Castleman, A. W., Jr *J. Chem. Phys.* **2003**, *118*, 9272. (b) Ikeda, T.; Fujiyoshi, S.; Kato, H.; Kudo, A.; Onishi, H. *J. Phys. Chem. B* **2006**, *110*, 7883. (c) Abe, R.; Sayama, K.; Sugihara, H. *J. Phys. Chem. B* **2005**, *109*, 16052.

(3) (a) Bonev, B. P.; Mumma, M. J.; DiSanti, M. A.; Dello Russo, N.; Magee-Sauer, K.; Ellis, R. S.; Stark, D. P. *Astrophys. J.* **2006**, *653*, 774. (b) Bonev, B. P.; Mumma, M. J.; Dello Russo, N.; Gibb, E. L.; DiSanti, M. A.; Magee-Sauer, K. *Astrophys. J.* **2004**, *615*, 1048. (c) Sandor, B. J.; Clancy, R. T. *J. Geophys. Res.* **2003**, *108*, 4463. (d) Yung, Y. L.; DeMore, W. B. *Photochemistry of Planetary Atmospheres*; Oxford University Press: New York, 1999.

(4) Hewitt, C. N. *Reactive Hydrocarbons in the Atmosphere*; Academic Press: San Diego, CA, 1999.

(5) *Chemistry and Radiation Changes in the Ozone Layer*; Zerefos, C. S., Isaksen, I. S. A., Ziomas, I., Eds.; NATO ASI Series, 557; Kluwer Academic Publishers: Dordrecht, The Netherlands, 2000.

(6) Cagin, S. *Between Earth and Sky: How CFCs Changed Our World and Endangered the Ozone Layer*; Pantheon: New York, 1993.

(7) Bar-Nun, A.; Dimitrov, V. *Icarus* **2006**, *181*, 320.

(8) (a) Kim, Y.; Dutta, P. K. *J. Phys. Chem. C* **2007**, *111*, 10575. (b) Zhang, J.; Du, P.; Schneider, J.; Jarosz, P.; Eisenberg, R. *J. Am. Chem. Soc.* **2007**, *129*, 7726. (c) Maeda, K.; Domen, K. *J. Phys. Chem. C* **2007**, *111*, 7851. (d) Lin, W.-H.; Cheng, C.; Hu, C.-C.; Teng, H. *Appl. Phys. Lett.* **2006**, *89*, 211904. (e) Maeda, K.; Teramura, K.; Lu, D.; Saito, N.; Inoue, Y.; Domen, K. *Angew. Chem., Int. Ed.* **2006**, *45*, 7806.

(9) (a) Sander, M. U.; Luther, K.; Troe, J. *Ber. Bunsen-Ges. Phys. Chem.* **1993**, *97*, 953. (b) Thomson, C. L.; Madsen, D.; Keiding, S. R.; Thøgersen, J.; Christiansen, O. *J. Chem. Phys.* **1999**, *110*, 3453.

(10) Okabe, H. *Photochemistry of Small Molecules*; Wiley: New York, 1978.

(11) Crowell, R. A.; Bartels, D. M. *J. Phys. Chem.* **1996**, *100*, 17940.

(12) (a) Han, P.; Bartels, D. M. *J. Phys. Chem.* **1992**, *96*, 4899. (b) Elles, C. G.; Shkrob, I. A.; Crowell, R. A.; Bradforth, S. E. *J. Chem. Phys.* **2007**, *126*, 164503.

(13) Hart, E. J.; Anbar, M. *The Hydrated Electron*; Wiley-Interscience: New York, 1971.

(14) Swallow, A. J. *Radiation Chemistry. An Introduction*; Longman: London, 1973.

(15) Hartig, K. J.; Getoff, N. *J. Photochem.* **1982**, *18*, 29.

(16) (a) Nikogosyan, D. N.; Oraevsky, A. A.; Rupasov, V. I. *Chem. Phys.* **1983**, *77*, 131. (b) Birkedal, V.; Madsen, E. S. Y.; Petersen, C.; Johnsen, M.; Seegert, A.; Jensen, S. K.; Keiding, S. R.; Thogersen, *J. Chem. Phys.* **2006**, *328*, 119.

(17) (a) Heller, J. M., Jr.; Hamm, R. N.; Birkoff, R. D.; Painter, L. R. *J. Chem. Phys.* **1974**, *60*, 3483. (b) Williams, F.; Varma, S. P.; Hillenius, S. *J. Chem. Phys.* **1976**, *64*, 1549.

(18) Goddard, W. A., III; Hunt, W. J. *Chem. Phys. Lett.* **1974**, *24*, 464.

(19) Dutit, O.; Tabche-Fouhaile, A.; Nenner, I.; Frochlich, H.; Guyon, P. M. *J. Chem. Phys.* **1985**, *83*, 584.

(20) (a) Kim, K. S.; Dupuis, M.; Lie, G. C.; Clementi, E. *Chem. Phys. Lett.* **1986**, *131*, 451. (b) Mhin, B.-J.; Kim, H. S.; Kim, H. S.; Yoon, J. W.; Kim, K. S. *Chem. Phys. Lett.* **1991**, *176*, 41. (c) Kim, K. S.; Mhin, B. J.; Choi, U.-S.; Lee, K. *J. Chem. Phys.* **1992**, *97*, 6649.

(21) Franken, K. A.; Jalaie, M.; Dykstra, C. E. *Chem. Phys. Lett.* **1992**, *198*, 59.

(22) (a) Pribble, R. N.; Zwier, T. S. *Science* **1994**, *265*, 75. (b) Pedulla, J. M.; Vila, F.; Jordan, K. D. *J. Chem. Phys.* **1996**, *105*, 11091. (c) Gruenloh, C. J.; Carney, J. R.; Arrington, C. A.; Zwier, T. S.; Fredericks, S. Y.; Jordan, K. D. *Science* **1997**, *276*, 1678.

(23) (a) Kim, J.; Kim, K. S. *J. Chem. Phys.* **1998**, *109*, 5886. (b) Kim, J.; Majumdar, D.; Lee, H. M.; Kim, K. S. *J. Chem. Phys.* **1999**, *110*, 9128. (c) Lee, H. M.; Suh, S. B.; Lee, J. Y.; Tarakeshwar, P.; Kim, K. S. *J. Chem. Phys.* **2000**, *112*, 9759.

(24) (a) Xantheas, S. S.; Dunning, T. H., Jr *J. Chem. Phys.* **1993**, *98*, 8037. (b) Fanourgakis, G. S.; Apra, E.; Xantheas, S. S. *J. Chem. Phys.* **2004**, *121*, 2655.

(25) Ojamäe, L.; Shavitt, I.; Singer, S. J. *J. Chem. Phys.* **1998**, *109*, 5547.

(26) (a) Graf, S.; Mohr, W.; Leutwyler, S. *J. Chem. Phys.* **1999**, *110*, 7893. (b) Klopper, W.; Luthi, H. P. *Mol. Phys.* **1999**, *96*, 559.

(27) (a) Milett, A.; Moszyński, R.; Wormer, P. E. S.; van der Avoird, A. *J. Phys. Chem. A* **1999**, *103*, 6811. (b) Gregory, J. K.; Clary, D. C. *J. Phys. Chem.* **1996**, *100*, 18014. (c) Severson, M. W.; Buch, V. *J. Chem. Phys.* **1999**, *111*, 10866. (d) Kim, K. S.; Tarakeshwar, P.; Lee, J. Y. *Chem. Rev.* **2000**, *100*, 4145. (e) Buck, U.; Huisken, F. *Chem. Rev.* **2000**, *100*, 3863.

(28) (a) Frisch, M. J.; Del Bene, J. E.; Binkley, J. S.; Schaefer III, H. F. *J. Chem. Phys.* **1986**, *84*, 2279. (b) Davidson, E. R.; Chakravorty, S. J. *Chem. Phys. Lett.* **1994**, *217*, 48. (c) Fowler, J. E.; Schaefer, H. F., III *J. Am. Chem. Soc.* **1995**, *117*, 446. (d) Valeev, E. F.; Schaefer, H. F., III *J. Chem. Phys.* **1998**, *108*, 7197.

(29) Werner, H.-J.; Knowles, P. J.; Lindh, R.; Manby, F. R.; Schütz, M.; Celani, P.; Korona, T.; Rauhut, G.; Amos, R. D.; Bernhardsson, A.;

Berning, A.; Cooper, D. L.; Deegan, M. J. O.; Dobbyn, A. J.; Eckert, F.; Hampel, C.; Hetzer, G.; Lloyd, A. W.; McNicholas, S. J.; Meyer, W.; Mura, M. E.; Nicklass, A.; Palmieri, P.; Pitzer, R.; Schumann, U.; Stoll, H.; Stone, A. J.; Tarroni, R.; Thorsteinsson, T. *MOLPRO*, version 2006.1, a package of ab initio programs. http://www.molpro.net.

(30) (a) Kołaski, M.; Lee, H. M.; Pak, C.; Dupuis, M.; Kim, K. S. *J. Phys. Chem. A* **2005**, *109*, 9419. (b) Timerghazin, Q. K.; Peslherbe, G. H. *J. Am. Chem. Soc.* **2003**, *125*, 9904. (c) Lee, H. M.; Kolaski, M.; Kim, K. S. *ChemPhyChem* **2008**, *9*, 567. (d) Kolaski, M.; Lee, H. M.; Pak, C.; Kim, K. S. *J. Am. Chem. Soc.* **2008**, *130*, 103.

(31) (a) Dupuis, M.; Marquez, A.; Davidson, E. R. *HONDO 99.6*, 1999, based on HONDO 95.3, Quantum Chemistry Program Exchange (QCPE), Indiana University, Bloomington, IN 47405.

(32) (a) Tachikawa, H. *J. Phys. Chem. A* **2002**, *106*, 6915. (b) Tachikawa, H. *J. Phys. Chem. A* **2004**, *108*, 7853.

(33) (a) Mulliken, R. S. *J. Chem. Phys.* **1955**, *23*, 1833. (b) Glendening, E. D.; Badenhoop, J. K.; Reed, A. E.; Carpenter, J. E.; Bohmann, J. A.; Morales, C. M.; Weinhold, F. *NBO 5.0 program*; University of Wisconsin: Madison, WI, 2001.

(34) (a) Eigen, M.; Maeyer, L. D. *Proc. R. Soc. London, Ser. A* **1958**, *247*, 505. (b) Zundel, G.; Metzer, H. *Z. Phys. Chem. (Munich)* **1968**, *58*, 225. (c) Shin, I.; Park, M.; Min, S. K.; Lee, E. C.; Suh, S. B.; Kim, K. S. *J. Chem. Phys.* **2006**, *125*, 234305. (d) Singh, N. J.; Park, M.; Min, S. K.; Suh, S. B.; Kim, K. S. *Angew. Chem., Int. Ed.* **2006**, *45*, 3795. (e) Jiang, J. C.; Wang, Y. S.; Chang, H. C.; Lin, S. H.; Lee, Y. T.; Niedner-Schatteburg, G.; Chang, H. C. *J. Am. Chem. Soc.* **2000**, *122*, 1398. (f) Tarakeshwar, P.; Choi, H. S.; Kim, K. S.; Djafari, S.; Buchhold, K.; Reimann, B.; Barth, H.-D.; Brutschy, B. *J. Chem. Phys.* **2001**, *114*, 4016. (g) Headrick, J. M.; Diken, E. G.; Walters, R. S.; Hammer, N. I.; Christie, R. A.; Cui, J.; Myshakin, E. M.; Duncan, M. A.; Johnson, M. A.; Jordan, K. D. *Science* **2005**, *308*, 1765.

(35) (a) Evangelisti, S.; Daudey, J. P.; Malrieu, J. P. *Phys. Rev. A* **1987**, *35*, 4930. (b) Nikolić, D.; Lindroth, E. *J. Phys. B: At. Mol. Opt. Phys.* **2004**, *37*, L285. (c) Kaldor, U. *Phys. Rev. A* **1988**, *38*, 6013.

JP711485B